A 3D optimization algorithm for sustainable cutting of slabs from ornamental stone blocks

Published Version:
Elkarmoty M., Bondua S., Bruno R. (2020). A 3D optimization algorithm for sustainable cutting of slabs from ornamental stone blocks. RESOURCES POLICY, 65, 1-11 [10.1016/j.resourpol.2019.101533].

Availability:
This version is available at: https://hdl.handle.net/11585/707296 since: 2019-12-03

Published:
DOI: http://doi.org/10.1016/j.resourpol.2019.101533

Abstract

Ornamental stones are natural building materials, extracted from quarries, which need to be cut and processed sustainably. Natural discontinuities adversely affect the sawing/cutting of blocks into commercial-size slabs. This work presents a 3D optimization algorithm for the sawing/cutting of ornamental stone blocks. The developed algorithm is based on 3D modeling of discontinuities as data input. The algorithm search for the intersection between a 3D cutting grid formed of a determined size of slabs and the model of discontinuities leading to calculate the recovery ratio considering several cutting orientations and displacements of the 3D cutting grid. The algorithm was coded in a program named SlabCutOpt that allows speed problem solving. SlabCutOpt was implemented on a real case study of a commercial-size limestone block extracted from a quarry in Italy. A number of 37 different commercial-sizes of slabs forming 37 cutting grids were tested to investigate the optimum results in geo-environmental direction (recovery ratio) and economic directions (revenue). The findings revealed that a certain slab size gave the optimum recovery ratio, whilst another slab size provided the optimum revenue.

Keywords:

Sustainable quarrying; 3D optimization algorithm; Dimension stone; Revenue optimization; Waste minimization

1. Introduction

Ornamental stones are natural non-renewable resources that have to be exploited and processed in an optimized way to minimize waste production and maximize revenue. It is just a third of the extracted stone raw material arrives to the global market as a finished product, whilst the twothirds remaining are waste, considering the worldwide average in the ornamental stones extraction [1]. Ornamental stones are considered as main economic resources for many countries overall the world [2]. Therefore, and since ornamental stones are natural non-renewable resources, they have to be extracted and processed sustainably for environmental and economic reasons.

The right exploitation of ornamental stone is crucial for any competitive economic growth roadmaps of countries aiming the sustainable development [3]. Environmental and economic sustainability strategies for ornamental stone industry is being studied in literature [4–7]. There are recent trends for stone waste recycling [8–11], but minimization of waste production during exploitation and processing is with more preferable impact environmentally and economically. Ornamental stones blocks are extracted from quarries. Blocks are cut to obtain slabs and tiles. The size of tiles and slabs depends on building and construction final applications. Slabs and tiles can be subjected to several types of surface treatment. From a commercial point of view, the main factor that define the commercial price is the dimension of slabs. In General, the larger the size of slabs, the selling price is higher.

Blocks are cut/sawed in processing plants using diamond disc saws, diamond blade saws, or gang-saws. Currently, the most used is multi-blades gang-saws that can cut a block to slabs with certain and specific thickness. Several previous work studied the cutting process of ornamental stones considering the sawability [12], the cutting energy consumption [13], and the sawing performance [14]. In this paper, we consider a further aspect that is needed to fulfil the sustainable development of the cutting/sawing process of ornamental stone blocks.

Discontinuities, fractures and bedding planes define the exploitability of commercial-size ornamental stone blocks from quarries [15]. Discontinuities not detected on the outcrops adversely affect the quality of ornamental stone blocks. The recovery ratio of the stone deposit depends strongly on these parameters. The possibility to detect structural weaknesses regions of ornamental stone blocks before cutting it is an environmental and economic important phase. The most common methods used in practice are the traditional observation based methods, which can lead to erroneous or non-reliable results. Nowadays, there is an unsatisfactory lack in the use of non-destructive methods for fracture detection in ornamental stone blocks.

A survey on fracture detection methods is provided in [16]. Among the used methods, the Ground Penetrating Radar (GPR), appeared to be a valid non-destructive method for discontinuities detection in ornamental stone quarries of different rock types [17–28].

With reference to the use of GPR in order to detect and model discontinuities and assessing of rock blocks, it worth to mention the works in [24,29–33]. However, in [32], it is possible to analyze the application of a 3D deterministic discontinuities model, to ornamental stone blocks, significant for the topic of this paper.

Previous works presented stochastic or geometric algorithms, aiming to analyze the fracture geometry and quantify the volume of the so called natural blocks, that are defined by the natural discontinuities planes [34–36]. The natural rock blocks geometry identification can be used for a preliminary reserves estimation in quarries, as in the case of the calculation of the maximum largest cuboid [37] or of the marketable block size [38] that fit into the natural rock blocks. The previously listed methods were based on the manual survey method of out-cropping discontinuities. The target of this paper can be achievable when hidden discontinuities can be detected and modeled as well. Identification of natural blocks and the maximum largest cuboid algorithms may not work well on the ornamental stone blocks scale, considering that on that scale planes of discontinuities may or mayn't be intersected at this small scale.

A number of works have considered the production optimization at quarry or bench scale [39–42], based on the mapping of fractures through the manual survey method. However, this paper considers the production optimization at a block scale through a new methodological approach, on the basis of a 3D deterministic modeling approach-based GPR that models fractures as 3D surfaces, not planes as typically modeled in literature. The method presented in this paper does not have a limitation to the number of fracture families and their restricted input parameters (dip angle and dip direction, spacing). It is worth mentioning the work of [43] that provided a geometrical design computation of optimum cutting shapes from polygonal boundary ornamental stone slabs.

Several open questions on production optimization during the cutting phase of slabs from a block are: (i) which dimensions of slabs/tiles to be cut? (ii) Which is the best orientation of block cutting (parallel to x-plane, y-plane, or z-plane)? and (iii) What is the optimum angle of slabs cut from a block? In order to answer these questions, this paper presents a 3D computational algorithm developed to optimize the cutting grid pattern of a block, starting from a 3D fracture modeling method presented in [17]. The developed algorithm was coded using the C++ programming language in a software package named SlabCutOpt. The software code SlabCutOpt allows the computation of the problem and the visualization of the results. Indeed, the latter atomizes the finding of the optimum design related to the cutting grid pattern of a block for each commercial slab size tested, providing the optimum recovery ratio. The paper presents the application of the SlabCutOpt code to a case study of a limestone block and discusses the optimization results. To the best of the authors' knowledge, this is the first attempt of a production optimization model at the block scale.

2. Method

2.1. The optimization algorithm

The developed 3D optimization algorithm generates a 3D cutting grid for a block. The 3D cutting grid represents the slabs with equal dimensions (dim_x, dim_y, dim_z), as shown in Fig. 1. The 3D cutting grid was built starting from the center of the block (C) with a specified number of cuts in three orthogonal directions: n_x, n_y, n_z. The specified dimensions cover the 3D domain of the block, during the whole run of the algorithm, using a number of slabs in a way that n_i *dim__> block dimension I, with i=x,y,z.. The block is described by the minimum and maximum Cartesian coordinates (x_min, x_max, y_min, y_max, and z_min: z_max).

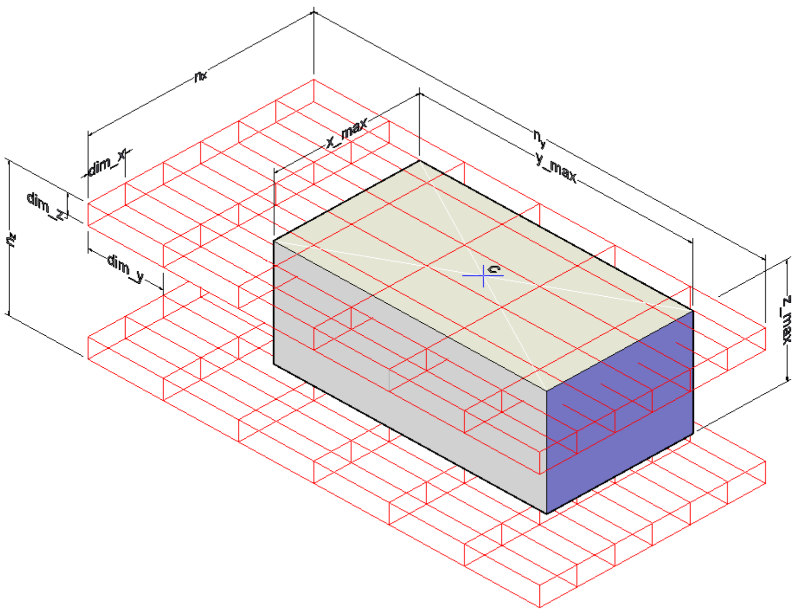

Fig. 1. Illustrative sketch showing the 3D cutting grid of the slabs (colored in red) within the block body.

The algorithm detects the intersection between the slabs (cutting grid) and the fractures model or the six faces of the block body. In this paper, the discontinuities model represents a model of fractures, joints, and voids. Iteratively, the cutting grid is rotated using a 3D rotation mode. The cutting orientations of the slabs can be parallel to the XY plane, XZ plane, or YZ plane of the block (see Fig. 2 and Table 1). The cutting grid is also subjected to several 3D displacements (dx, dy, dz), defined by Eq. (1), Eq. (2), and Eq. (3).

Commentato [SB1]: I addes plural. Is correct?

$$(-dim\_x)/2 \leq dx < (+dim\_x)/2, \text{ with a step of } dx\_step, \text{ for } dx \quad (1)$$

$$(-dim\_y)/2 \leq dy < (+dim\_y)/2, \text{ with a step of } dy\_step, \text{ for } dy \quad (2)$$

$$(-dim\_z)/2 \le dz < (+dim\_z)/2\text{, with a step of } dz\_step\text{, for } dz \qquad (3)$$

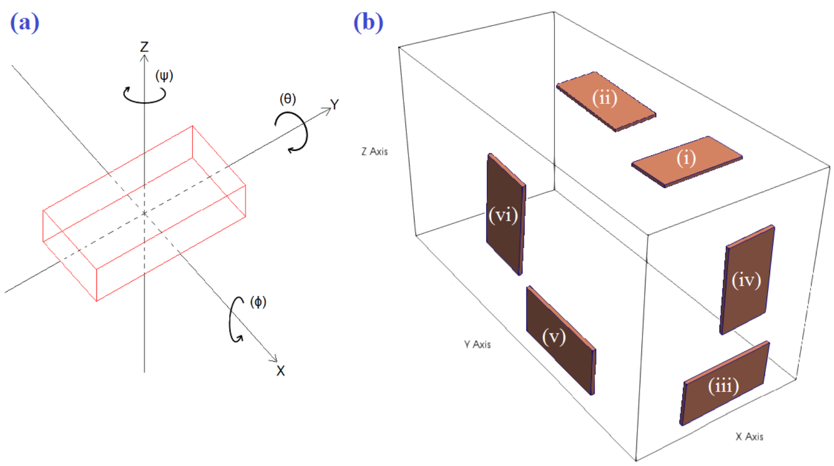

Fig. 2. (a) The possible orientation-rotation angles of the 3D cutting grid of the slabs; (b) A sketch showing the possible orientation-rotations within a block (details of the sub-figures numbering are given in Table 1).

Table 1
The possible orientations-rotations of the cutting grid.

cutting orientation of slabs	rotation of slabs	the relative orientation-rotation			figure
		theta θ	phi ϕ	psi ψ	
XY plane	0.0°	0.0°	0.0°	0.0°	Fig. 2b(i)
XY plane	90.0°	0.0°	0.0°	90.0°	Fig. 2b(ii)
XZ plane	0.0°	90.0°	0.0°	0.0°	Fig. 2b(iii)
XZ plane	90.0°	90.0°	90.0°	0.0°	Fig. 2b(iv)
YZ plane	0.0°	90.0°	0.0°	90.0°	Fig. 2b(v)
YZ plane	90.0°	90.0°	90.0°	90.0°	Fig. 2b(vi)

The intersection between a slab and a discontinuity (or with the faces of the block body) is detected by using a segment/triangle intersection algorithm [44]. The segment/triangle intersection algorithm [44] compute the signs of 4 determinants and don't require any explicit constructions that can be subject to numerical errors. Each discontinuity and the faces of the block body are geometrically defined by 3D triangles. For each 3D cutting grid patterns, each slab is checked if it intersects a discontinuity or a face of the block. This implies that a slab that is composed by 12 edge segments, the algorithm checks the intersection between the 12 edge segments and all the triangles that represent the discontinuities model. The algorithm computes the number of non-intersected slabs and total number of slabs (intersected + non-intersected) within the block body. The recovery ratio is calculated for each displacement and for each orientation-rotation to determine the optimum cutting grid pattern using Eq. (4). The recovery ratio is also called coefficient of utilization as given and defined in [45]. The recovery ratio described in Eq. (4) is limited to a fixed slab size as defined by the user. The SlabCutOpt algorithm consider a regular cutting grid, because the use of several slab sizes at the same time (irregular cutting grid), can theoretically provide higher recovery ratio, but a grid of several different sizes of slabs cut from a block can be hardly/practically carried out within the typical cutting process of ornamental stone blocks. Considering also that small non-commercial sizes of slabs may be included in the cutting grids. In most cases, the quarrymen cut a block to produce a specific size of slabs which the markets already need. However, in this paper, we aimed at comparing the results of several cutting grids comparing several slab size.

$$recovery\ (\%) = \frac{volume\ of\ non{-}intersected\ slabs\ with\ full\ dimension\ inside\ the\ block\ body\ x\ 100}{total\ volume\ of\ the\ block\ body} \quad (4)$$

In the processing plants, the cutting saws work with a continuous water flow that is required for cooling and reducing the dust emissions caused by sawing. The dust is the material lost during sawing which can be then reused for further applications [46–49]. The algorithm presented in this paper takes into account the thickness of the cutting saw and the volume of material lost/wasted due to sawing.

2.2. Software development

The developed algorithm was coded using the C++ programming language and makes use of the OpenMP library for multithreading computations. The software package developed was named “SlabCutOpt” on the basis of the algorithm aim: Slab Cutting Optimization.

2.2.1. Input data files

The input data of SlabCutOpt is composed of several files:

• SlabCutOpt.par: ASCII file containing the input parameters of cutting grid. It has to contain the geometric dimensions of the block body, the parameters about orientation-rotation and displacement and options concerning the operating mode and the output mode, etc. The algorithm can also work only in 2D, avoiding testing for the Z direction. See Appendix A for details;

• PLY files: each discontinuity or set of discontinuities has to modelled in one or more file using the polygon file format (ply) [50]. See Appendix B for details;

• PLY_FileList.dat: this is the ASCII file with the list of the ply files. See Appendix C for details.

• slab_dimensions.dat: this is the ASCII file contains the list of the several sizes of slabs to be tested. See Appendix D for details.

2.2.2. Files of results

The results files of SlabCutOpt are ASCII files with detailed information on the computations of the grid cutting optimization search, in addition to files needed for the 3D visualization. The results files of SlabCutOpt are:

•Results.log file: this is an ASCII file, where each row contains, for each slab size, the orientation of the 3D cutting grid, the applied displacements, the number of non-intersected slabs inside the block body, and the number of intersected slabs inside the block body. See Appendix E for details.

•slabs vtu files: optionally, a set of vtu files are generated for the 3D visualization of the cutting grid. The vtu file generation can be the whole set of cutting grids scenarios or just for the best solution (maximum number of non-intersected slabs). A slab type code is assigned to each slab, in the vtu files, to allow an easy visual perception of the kind of slab: out bounding of the block, intersected and non-intersected slabs. The vtu files can be then visualized using, for example, the free and open source visualization software ParaView [51]. Fig. 3 shows a schematic diagram of the software package structure.

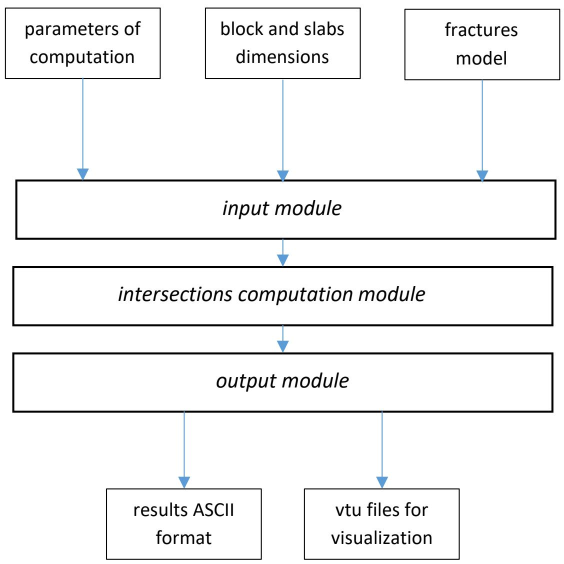

Fig. 3. A schematic diagram of SlabCutOpt software structure.

3. Case study

SlabCutOpt was applied to a real case study. The rock type of the commercial size block under study (1.55 m x 2.9 m x 1.10 m) was compacted limestone with a creamy-white color. It is a highly fractured limestone block whose out-cropping fractures and furthermore discontinuities could be detected and deterministically modeled as 3D surfaces based on GPR survey, this model of discontinuities and description of the block under study is presented in [32].

The revenue estimation of the block was carried out on the basis of a Relative Money Value (RMV) for each slab size, calculated by Eq. (5) (given that the real selling prices are confidential):

RMV for a slab = the slab selling price (€) / the maximum unit price of all the slabs (€) (5)

Table 2 presents the selected commercial sizes of the slabs with their RMV and surface area. A quasi linear correlation between the size (area) of the slabs and the commercial price was clearly found (Figure 4). The optimization solutions were investigated by SlabCutOpt for the whole commercial-sizes of the slabs listed in Table 2.

Table 2
The RMV of the commercial-sizes of slabs tested.

size No.	dimensions of slabs and tiles			RMV per unit	surface area (m^2)
	x (cm)	y (cm)	z (cm)		
size 1	40.00	20.00	1.50	0.082	0.08
size 2	50.00	25.00	1.50	0.127	0.13
size 3	40.00	20.00	2.00	0.087	0.08
size 4	50.00	25.00	2.00	0.136	0.13
size 5	60.00	30.00	1.50	0.207	0.18
size 6	30.00	30.00	1.50	0.104	0.09
size 7	40.00	40.00	1.50	0.184	0.16
size 8	60.00	45.00	1.50	0.311	0.27
size 9	45.00	45.00	1.50	0.233	0.20
size 10	48.00	48.00	1.50	0.265	0.23
size 11	60.00	30.00	2.00	0.219	0.18
size 12	30.00	30.00	2.00	0.110	0.09
size 13	40.00	40.00	2.00	0.195	0.16
size 14	60.00	45.00	2.00	0.329	0.27
size 15	45.00	45.00	2.00	0.246	0.20
size 16	48.00	48.00	2.00	0.280	0.23
size 17	80.00	40.00	1.50	0.442	0.32
size 18	80.00	48.00	1.50	0.531	0.38
size 19	80.00	40.00	2.00	0.463	0.32
size 20	80.00	48.00	2.00	0.556	0.38
size 21	30.50	30.50	1.00	0.107	0.09
size 22	30.00	15.00	3.00	0.040	0.05
size 23	30.00	10.00	3.00	0.027	0.03
size 24	30.00	110.00	2.00	0.380	0.33
size 25	35.00	150.00	2.00	0.604	0.53
size 26	40.00	190.00	2.00	0.875	0.76
size 27	30.00	110.00	3.00	0.434	0.33
size 28	35.00	150.00	3.00	0.691	0.53
size 29	40.00	190.00	3.00	1.000	0.76
size 30	15.00	60.00	2.00	0.098	0.09
size 31	20.00	80.00	2.00	0.174	0.16
size 32	25.00	100.00	2.00	0.271	0.25
size 33	25.00	125.00	2.00	0.339	0.31
size 34	15.00	60.00	3.00	0.104	0.09
size 35	20.00	80.00	3.00	0.184	0.16
size 36	25.00	100.00	3.00	0.288	0.25
size 37	25.00	125.00	3.00	0.360	0.31

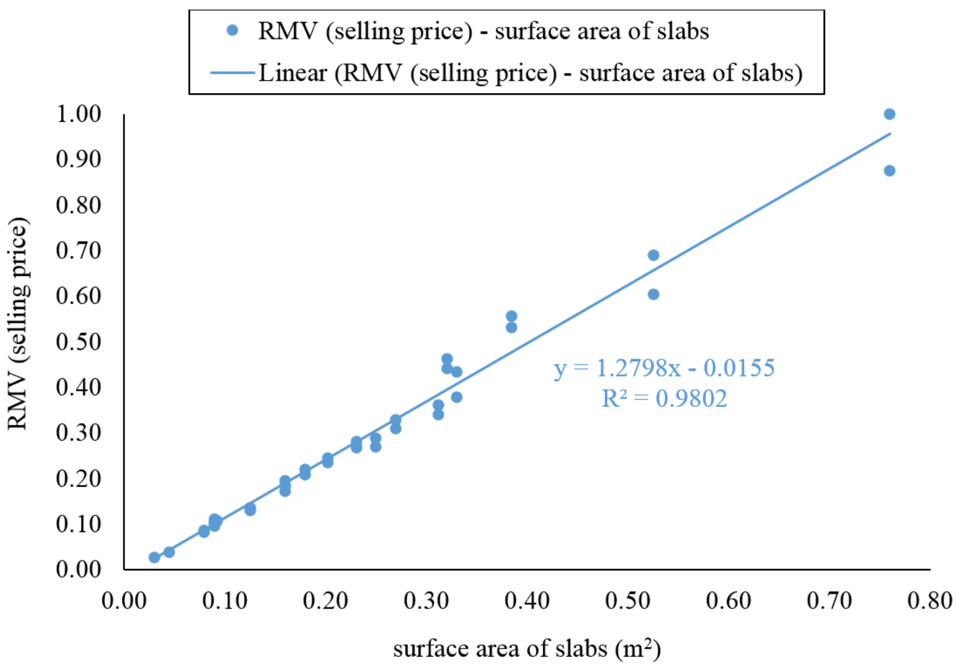

Fig. 4. Correlation between the sizes of the slabs and the RMV.

4. Results

For each slab size of Table 2, a 3D cutting grid was used to compute the non-intersected slabs, using the six orientations-rotations and several displacements of the cutting grid. The algorithm parameters used in this study (SlabCutOpt.par file) are presented in Appendix A. Fig. 5 shows, for slab size No. 1 of Table 2, the computation results of several simulated 3D cutting grids. For clarity, the discontinuities inside the limestone block body are represented using the same colors as in the model presented in [32]. The cutting saw thickness is clearly visible in Fig. 5g and Fig 5h, as the slabs are separated from each others. Fig. 5h simplifies graphically the intersection and calculation methodology within a single discontinuity.

The results of the slab No. 1 (size 40.0 cm x 20.0 cm x 1.50 cm) are given in Fig. 6. For this cutting grid scenario, the optimum recovery ratio was found to be 35.7 %. For this size, the optimum cutting orientation is parallel to the plane XY – slab rotation 0.0° and with a displacement of (dx = -0.01 m, dy = 0.1 m, dz = -0.01 m). From Fig. 6, it can be observed that the recovery ratio varies within each single orientation-rotation as well as between the six orientations-rotations.

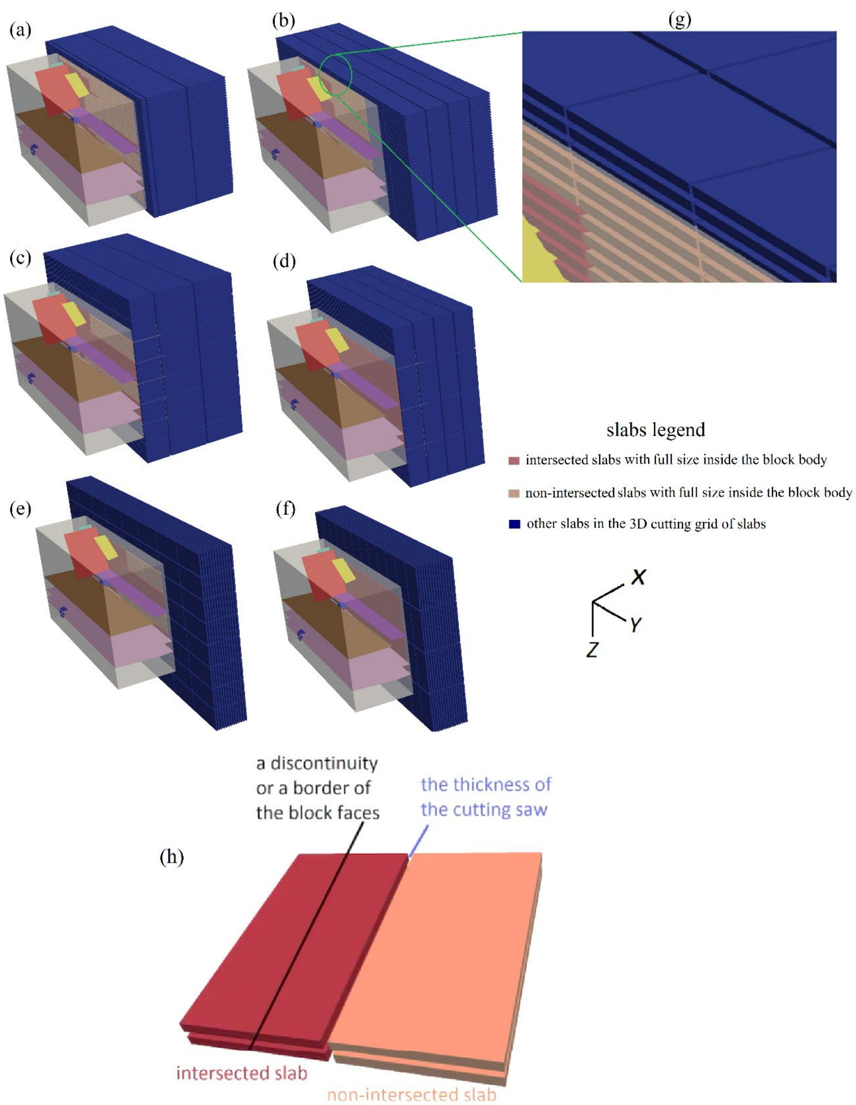

Fig. 5. The 6 orientations/rotations (sub-figures a, b, c, d, e, and f) of the cutting grid scenario using ParaView. This figure refers to the results of slab size No. 1. Details of the sub-figures a, b, c, d, e, and f are provided in Table 3. Sub-figures g and h are illustrative figures.

Table 3

The sub-figures details presented in Fig. 5.

sub-figure	cutting orientation of the slabs	rotation of the slabs
Fig. 4a	XY plane	0.0°
Fig. 4b	XY plane	90.0°
Fig. 4c	XZ plane	0.0°
Fig. 4d	XZ plane	90.0°
Fig. 4e	YZ plane	0.0°
Fig. 4f	YZ plane	90.0°

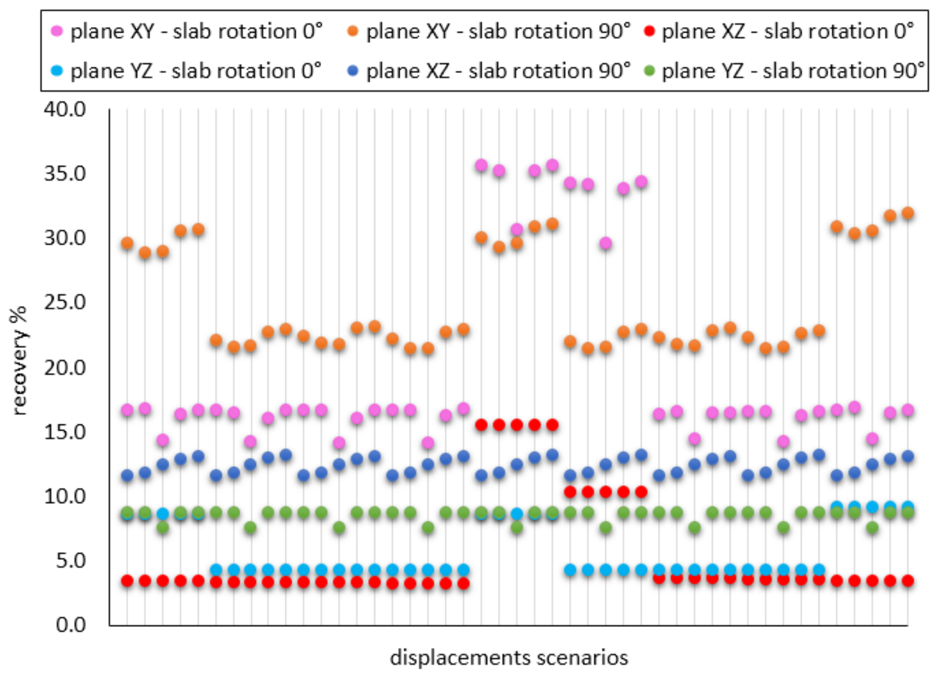

Fig. 6. Graphical representation of the optimization results for the slab size No. 1.

The maximum number of non-intersected slabs and the maximum recovery ratio for each tested slab size are represented in Fig. 7. The best recovery ratio of 44.91 % was found for the cutting grid of the slab size No. 23. The cutting orientation is parallel to plane XY – slab rotation 90.0°, with a displacement of (dx = -0.01 m, dy = 0.05 m, dz = -0.02 m), which can be taken as the most environmental friendly solution. From Fig. 7, the histogram of the maximum recovery is not in agreement with the maximum number of non-intersected slabs. In fact, for example, the maximum recovery ratio for the slab size No. 13 is higher than for slab size No. 12. However, the maximum number of non-intersected slabs for the cutting grid of slab size No. 13 is lower than for slab size No. 12. This is because the volumes of slabs are different and the volume controls the recovery ratio.

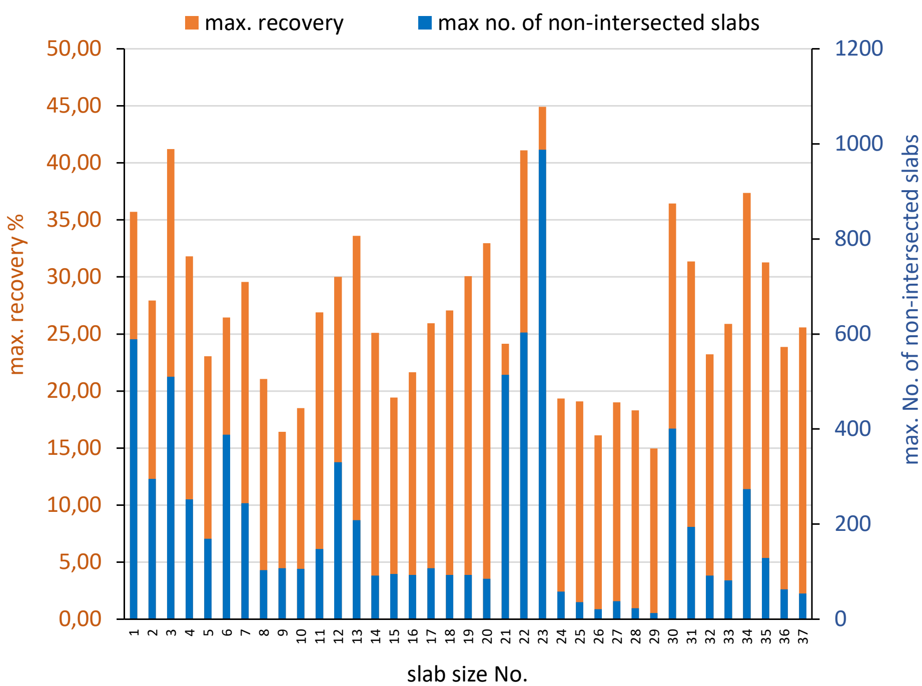

Fig. 7. Maximum recovery ratio and maximum number of non-intersected slabs for all sizes of slabs .

From an economic point of view, neither the maximum recovery ratio nor the maximum number of non-intersected slabs can be used as comparison indicator for the cutting grid optimization within a range of different slab sizes. When several sizes are considered, the total revenue calculated by Eq. (6) can be a more effective comparison indicator to assess the optimum solution.

$$revenue = number\ of\ non\ intersected\ slabs\ \times RMV\ per\ unit \tag{6}$$

Interestingly, as shown in Fig. 8, the optimal (maximum) revenue is then obtained from the cutting grid scenario No. 21 with a total revenue value of 55.0 RMV. Neither the maximum number of non-intersected slabs nor the maximum recovery ratio could be found in this slab size. This imply that, the final economical solution (maximum RMV), given by SlabCutOpt, for this block, was identified in slab size No. 21, at the cutting orientation parallel to plane XY – slab rotation 0° with a displacement: (dx = -0.11 m, dy = 0.04 m, dz = -0.01), and equally at the cutting orientation parallel to plane XY – slab rotation 90° with a displacement: (dx = -0.11 m, dy = 0.04 m, dz = -0.01). These results were expected since the slab is square-shaped (30.5 cm x 30.5 cm), therefore, the slab rotation had no effect on the final results. Fig. 9 shows a 3D clip visualization of the final optimal economical solution (slab size No. 21).

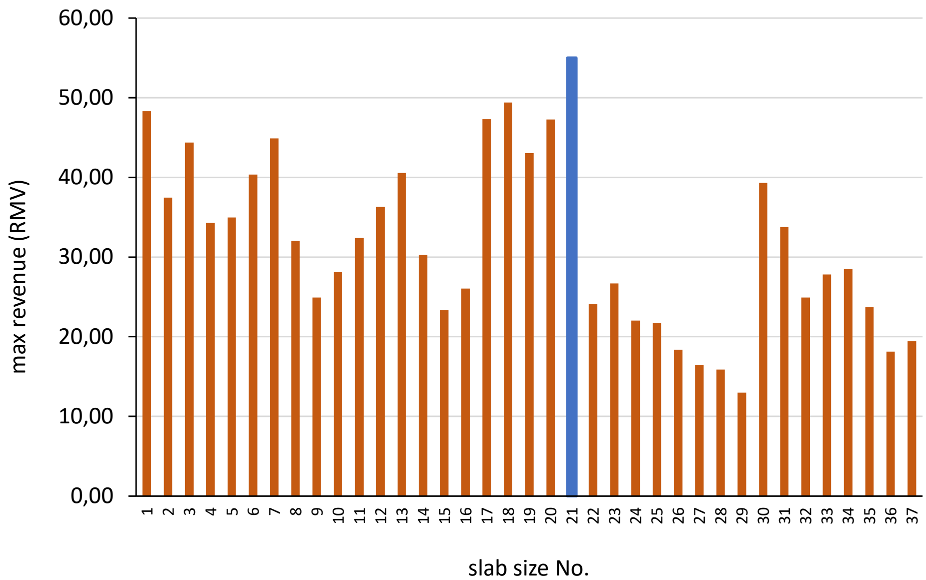

Fig. 8. The maximum revenue obtained for each slab size.

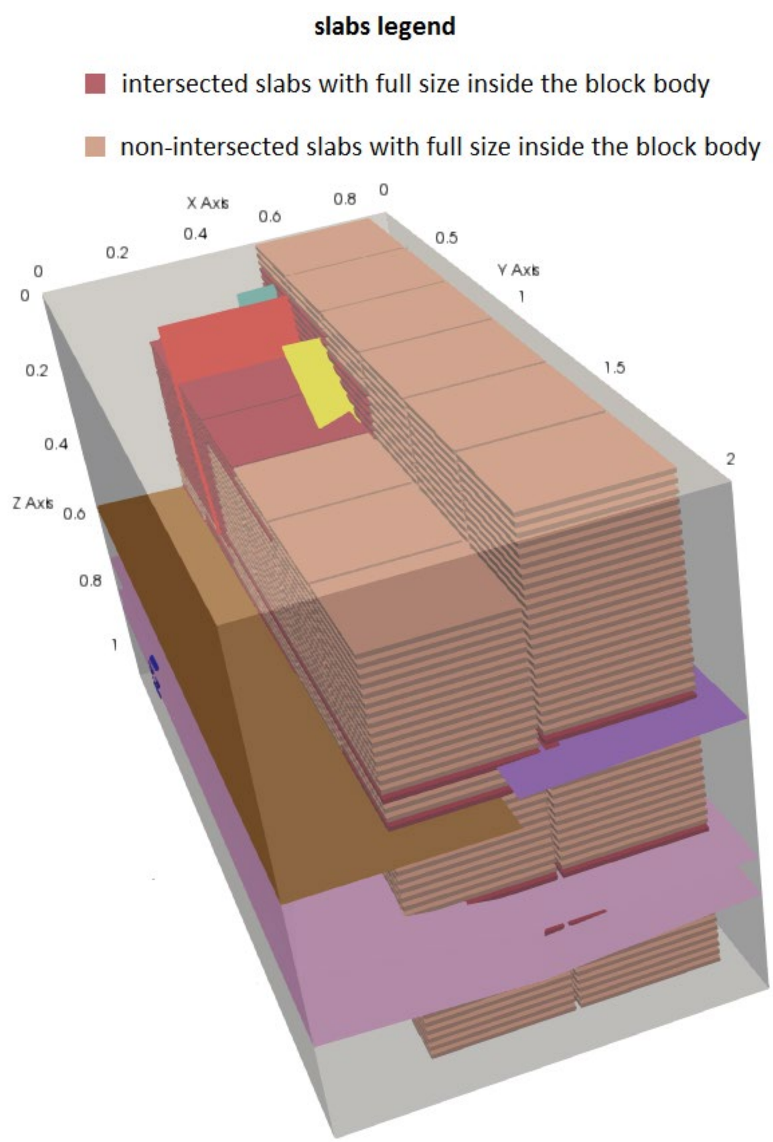

Fig. 9. A 3D clipped view of the optimal economical solution visualized using ParaView.

The grain texture or pattern of an ornamental stone product is an important commercial characteristic. The final product aesthetic pleasure is taken in account when the block is cut for applications of prestigious and decoration purposes. The rotation of the cutting grid may cause a change of the final texture of the ornamental stone product in case of stones with veins or color gradation patterns. The presented algorithm can be used for stones which have a uniform color with a texture that is insensitive to the grid rotation and for materials used for building and construction applications that do not concern with texture. It was referred to such these cases of possible rotation of the cutting pattern also by [43]. If the commercial value of the slabs is known (or can be estimated) for different cutting orientation/rotation, then it is still possible to estimate the total revenue for each cutting grid scenario.

The surface area of the slabs tested, in the case study, played a main role in the run of SlabCutOpt software. The maximum number of non-intersected slabs, is strongly correlated in a negative power relation with the surface area value of the slabs (Fig. 10). When information about the commercial price for other non-tested slab sizes in SlabCutOpt is available, the use of the correlation formula (in Fig. 10) can be used to estimate their relative revenue. However, SlabCutOpt will still be needed in order to know the relative geometric design of the optimum cutting orientation-rotation of slabs.

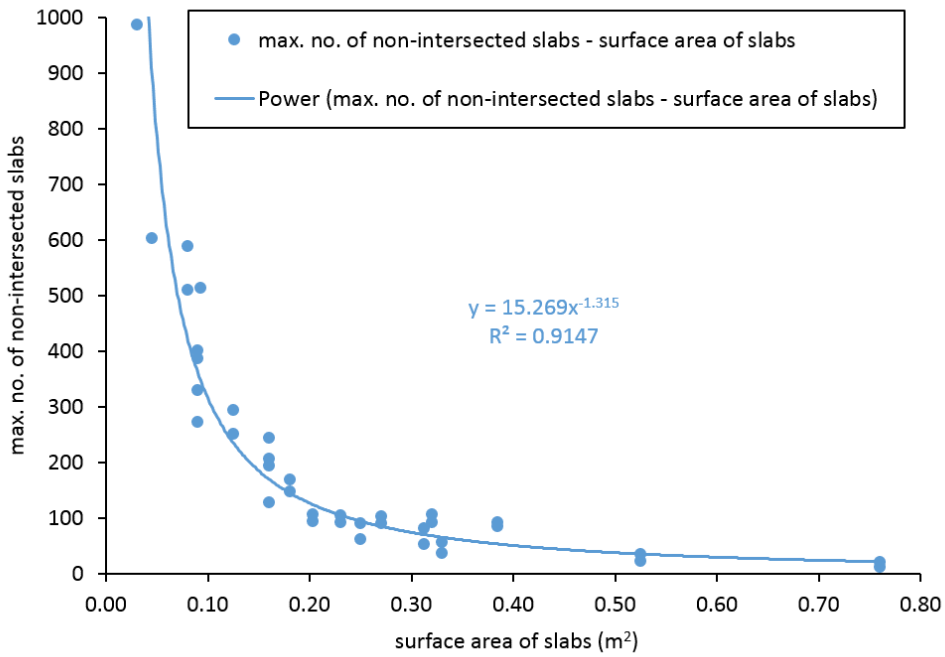

Fig. 10. The relation between the surface area of slabs and the number of non-intersected slabs obtained for each size.

The computation time of the SlabOptCut run (considering parameter write_vtu=1, see Appendix A), on a personal computer equipped with a 64-bit operative system Windows 10, a processor Intel i7-3770K CPU @ 3.5 GHz , and an installed memory (RAM) of 8.00 GB, was 23.0 minutes. Depending by the kind of application, the computation time strongly depends on Input/Output files operations. Avoiding time consuming operation of printing out vtu files for each simulated cutting grid, the computation time was reduced up to to 37.0 seconds (considering parameter write_vtu=2, see Appendix A). The SlabCutOpt algorithm used the OpenMP[52] library to compute the number of no-intersected slab for different scenarios simultaneously using several threads for fast computation.

5. Conclusions

Cutting scenarios (3D cutting grid patterns) of a stone block could be tested using the presented software code SlabCutOpt to optimize the recovery ratio or the revenue of the block. We developed a 3D optimization algorithm to simulate several 3D cutting scenarios of slabs. Discontinuities need to be modeled for the whole volume of the ornamental stone block. For each 3D cutting scenario, the algorithm calculates the number of non-intersected slabs - with discontinuities or the block body borders - which allowed calculating the recovery ratio. The optimization algorithm SlabCutOpt was successfully coded in C++ and allowed to visualize the optimized result in 3D using a data visualization software package, such as ParaView.

The presented algorithm can work with discontinuities data described in PLY files whatever the detection method is. In the presented case study, the results was based on modeling discontinuities, as 3D surfaces, detected by GPR survey, as recommended by the authors. However, the obtained results are subjected to the limitations of the GPR method. If a tinny hidden fracture could not be detected, it may lead to have unconsidered fractured slab, particularly when it is open fracture. Therefore, using more than a method for fracture detection or more than one GPR frequency (higher) can increase the accuracy of the discontinuities model.

For the presented case study of a limestone block, among 37 several -sizes of slabs, the cutting grid of slab size No. 23 of dimensions 30.0 cm x 10.0 cm x 3.0 cm provided the optimum production recovery ratio. Furthermore, economic factors have to be taken into account to correctly evaluate the optimal solution of the cutting grid scenario. Slab size No. 21 of dimensions 30.5 cm x 30.5 cm x 1.0 cm provided the final optimal economical solution.

A negative power correlation was found between the maximum number of the non-intersected slabs and the surface area of slabs. This correlation can be used, for example, to estimate the maximum number of non-intersected slabs for other cutting grid sizes.

SlabCutOpt is recommended to be used in quarrying companies to maximize recovery and revenue, it can provide stone processing factories with the slab sizes optimize the revenue and minimize the waste. Moreover, SlabCutOtp allows quarrying companies to study the potential revenue value of various slab sizes products enabling quarrying companies to estimate the revenue and recovery when commitment with customers exists regarding certain slab sizes. Waste material quantity and size can be estimated using SlabCutOpt allowing further studying of waste re-processing and recycling potential.

Future works include the considerations of the cutting cost, energy consumption, and material texture preference in the algorithm. A comparison study between the computed cutting patterns by SlabCutOpt and the actual cutting results of a stone block at a processing plant is recommended. A combination of non-destructive fracture detection and modeling techniques and SlabCutOpt is recommended for environmental and economic sustainable reasons.

Acknowledgements

The authors are grateful to Michele Augelli, “Augelli Marmi” quarrying company, for allowing the GPR test and to Carlo Cormio (SERENGEO Srl, a spin-off company of the University of Bologna) for the technical suggestions provided. A special word of thanks goes to the EU-METALIC II—

ERASMUS MUNDUS program that funded the lead author’s PhD scholarship. Many thanks to the Italian Ministry of Foreign Affairs and International Cooperation for funding this research, enabling to improve and continue the research topic in this paper.

References

[1] C. Montani, Stone 2002—world marketing handbook, Gruppo Editoriale Faenza Editice., Faenza, Italy, 2003.

[2] C. Montani, Stone 2008—world marketing handbook., Faenza, Gruppo Editoriale Faenza Editice, Faenza, 2008.

[3] J. Carvalho, C. Lopes, A. Mateus, L. Martins, M. Goulão, Planning the future exploitation of ornamental stones in Portugal using a weighed multi-dimensional approach, Resour. Policy. 59 (2018) 298–317. doi:10.1016/j.resourpol.2018.08.001.

[4] N. Careddu, Dimension stones in the circular economy world, Resour. Policy. 60 (2019) 243–245. doi:10.1016/j.resourpol.2019.01.012.

[5] D. Macedo, R. Mori, A. Maria, P. Mizusaki, Sustainability strategies for dimension stones industry based on Northwest region of Espírito Santo State , Brazil, Resour. Policy. 52 (2017) 207–216. doi:10.1016/j.resourpol.2017.03.005.

[6] N. Careddu, G. Siotto, R. Siotto, C. Tilocca, From land fi ll to water, land and life : The creation of the Centre for stone materials aimed at secondary processing, Resour. Policy. 38 (2013) 258–265. doi:10.1016/j.resourpol.2013.05.001.

[7] N. Careddu, G. Siotto, Promoting ecological sustainable planning for natural stone

quarrying . The case of the Orosei Marble Producing Area in Eastern Sardinia, Resour. Policy. 36 (2011) 304–314. doi:10.1016/j.resourpol.2011.07.002.

[8] M. Galetakis, G. Alevizos, K. Leventakis, Evaluation of fine limestone quarry by-products, for the production of building elements - An experimental approach, Constr. Build. Mater. 26 (2012) 122–130. doi:10.1016/j.conbuildmat.2011.05.011.

[9] M. Galetakis, A. Soultana, A review on the utilisation of quarry and ornamental stone industry fine by-products in the construction sector, Constr. Build. Mater. J. 102 (2016) 769–781. doi:10.1016/j.conbuildmat.2015.10.204.

[10] G. Marras, N. Careddu, Sustainable reuse of marble sludge in tyre mixtures, Resour. Policy. 59 (2018) 77–84. doi:10.1016/j.resourpol.2017.11.009.

[11] A. Cavallo, Serpentinitic waste materials from the dimension stone industry : Characterization, possible reuses and critical issues, Resour. Policy. 59 (2018) 17–23. doi:10.1016/j.resourpol.2018.08.003.

[12] D. Tumac, A. Shaterpour-Mamaghani, Estimating the sawability of large diameter circular saws based on classification of natural stone types according to the geological origin, Int. J. Rock Mech. Min. Sci. 101 (2018) 18–32. doi:10.1016/j.ijrmms.2017.11.014.

[13] M. Yurdakul, K. Gopalakrishnan, H. Akdas, Prediction of specific cutting energy in natural stone cutting processes using the neuro-fuzzy methodology, Int. J. Rock Mech. Min. Sci. 67 (2014) 127–135. doi:10.1016/j.ijrmms.2014.01.015.

[14] A. Aryafar, R. Mikaeil, S. Shaffiee, S. Shaffiee, Utilization of soft computing for evaluating

the performance of stone sawing machines , Iranian quarries, Int. J. Min. Geo-Engineering. in press (2018). doi:10.22059/IJMGE.2017.233493.594673.

[15] J.F. Carvalho, P. Henriques, P. Falé, G. Luís, Decision criteria for the exploration of ornamental-stone deposits: Application to the marbles of the Portuguese Estremoz Anticline, Int. J. Rock Mech. Min. Sci. 45 (2008) 1306–1319. doi:10.1016/j.ijrmms.2008.01.005.

[16] M. Elkarmoty, C. Colla, E. Gabrielli, S. Bonduà, R. Bruno, A combination of GPR survey and laboratory rock tests for evaluating an ornamental stone deposit in a quarry bench, Procedia Eng. 191 (2017) 999–1007. doi:10.1016/j.proeng.2017.05.272.

[17] M. Elkarmoty, C. Colla, E. Gabrielli, S. Bonduà, R. Bruno, Deterministic three-dimensional rock mass fracture modeling from geo-radar survey: a case study in a sandstone quarry in Italy, Environ. Eng. Geosci. 23 (2017) 314–331. doi:10.2113/gseegeosci.23.4.314.

[18] M. Elkarmoty, C. Colla, E. Gabrielli, S. Kasmaeeyazdi, F. Tinti, S. Bonduà, R. Bruno, Mapping and modelling fractures using ground penetrating radar for ornamental stone assessment and recovery optimization: Two case studies, Mining-Geological-Petroleum Eng. Bull. 32 (2017) 63–76. doi:10.17794/rgn.2017.4.7.

[19] J. Martínez, V. Montiel, J. Rey, F. Cañadas, P. Vera, Utilization of Integrated Geophysical Techniques to Delineate the Extraction of Mining Bench of Ornamental Rocks (Marble), Remote Sens. 9 (2017) 1322. doi:10.3390/rs9121322.

[20] M. Elkarmoty, F. Tinti, S. Kasmaeeyazdi, F. Giannino, S. Bonduà, R. Bruno, Implementation

of a fracture modeling strategy based on georadar survey in a large area of limestone quarry bench, Geosciences. 8 (2018) 1–15. doi:10.3390/geosciences8120481.

[21] S.J. Seol, J.-H. Kim, Y. Song, S.-H. Chung, Finding the strike direction of fractures using GPR, Geophys. Prospect. 49 (2001) 300–308. doi:10.1046/j.1365-2478.2001.00262.x.

[22] H. Luodes, H. Sutinen, P. Härmä, H. Pirinen, O. Selonen, Assessment of potential natural stone deposits, in: L.F. Lollino G., Manconi A., Guzzetti F., Culshaw M., Bobrowsky P. (Ed.), Eng. Geol. Soc. Territ. - Vol. 5, Springer, Cham, 2015: pp. 243–246. doi:10.1007/978-3-319-09048-1_47.

[23] H. Luodes, H. Sutinen, Evaluation and modelling of natural stone rock quality using Ground Penetrating Radar (GPR), in: Nenonen, K., Nurmi P.A. (Eds.), Geosci. Soc. 125th Anniv. Vol. Geol. Surv. Finland, Spec. Pap. 49, 2011: pp. 83–90.

[24] J. Rey, J. Martínez, P. Vera, N. Ruiz, F. Cañadas, V. Montiel, Ground-penetrating radar method used for the characterisation of ornamental stone quarries, Constr. Build. Mater. 77 (2015) 439–447. doi:10.1016/j.conbuildmat.2014.12.076.

[25] M. Lualdi, L. Zanzi, 2D and 3D experiments to explore the potential benefit of GPR investigations in planning the mining activity of a limestone quarry, in: Tenth Int. Conf. Gr. Penetrating Radar, GPR2004, 2004: pp. 613–616.

[26] B. Koster, F. Kruse, The use of ground penetrating radar (GPR) in the investigation of historical quarry abandonment in Svalbard, Polar Rec. (Gr. Brit). 52 (2016) 330–344. doi:10.1017/S0032247415000844.

[27] M. Grasmueck, R. Weger, H. Horstmeyer, Three-dimensional ground-penetrating radar imaging of sedimentary structures, fractures, and archaeological features at submeter resolution, Geology. 32 (2004) 933. doi:10.1130/G20776.1.

[28] M. Yi, J. Kim, S. Cho, M. Sato, Integrated application of borehole radar reflection and resistivity tomography to delineate fractures in granite quarry mine, in: Tenth Int. Conf. Gr. Penetrating Radar, 21-24 June, Delft, The Netherlands, 2004: pp. 213–216.

[29] L. Zanzi, A. Hojat, H. Ranjbar, S. Karimi-Nasab, A. Azadi, D. Arosio, GPR measurements to detect major discontinuities at Cheshmeh-Shirdoosh limestone quarry, Iran, Bull. Eng. Geol. Environ. (2017). doi:10.1007/s10064-017-1153-x.

[30] D. Arosio, S. Munda, L. Zanzi, Quality control of stone blocks during quarrying activities, in: 14th Int. Conf. Gr. Penetrating Radar, 4-8 June 2012, Shanghai, China, 2012: pp. 822–826. doi:10.1109/ICGPR.2012.6254975.

[31] D. Arosio, Rock fracture characterization with GPR by means of deterministic deconvolution, J. Appl. Geophys. 126 (2016) 27–34. doi:10.1016/j.jappgeo.2016.01.006.

[32] M. Elkarmoty, F. Tinti, S. Kasmaeeyazdi, S. Bonduà, R. Bruno, 3D modeling of discontinuities using GPR in a commercial size ornamental limestone block, Constr. Build. Mater. 166 (2018) 81–86. doi:10.1016/j.conbuildmat.2018.01.091.

[33] J. Rey, J. Martínez, V. Montiel, F. Cañadas, N. Ruiz, Characterization of the sedimentary fabrics in ornamental rocks by using GPR, Near Surf. Geophys. 15 (2017) 457–465. doi:10.3997/1873-0604.2017015.

[34] A. Turanboy, A geometric approach for natural rock blocks in engineering structures, Comput. Geosci. 14 (2010) 565–577. doi:10.1007/s10596-009-9171-9.

[35] A. Turanboy, E. Ülker, LIP-RM: An attempt at 3D visualization of in situ rock mass structures, Comput. Geosci. 12 (2008) 181–192. doi:10.1007/s10596-007-9077-3.

[36] R. Yarahmadi, R. Bagherpour, R. Kakaie, N.H. Mirzaie, M. Yari, Development of 2D computer program to determine geometry of rock mass blocks, Int. J. Min. Sci. Technol. 24 (2014) 191–194. doi:10.1016/j.ijmst.2014.01.008.

[37] E. Ülker, A. Turanboy, Maximum volume cuboids for arbitrarily shaped in-situ rock blocks as determined by discontinuity analysis—A genetic algorithm approach, Comput. Geosci. 35 (2009) 1470–1480. doi:10.1016/j.cageo.2008.08.017.

[38] M. Mutlutürk, Determining the amount of marketable blocks of dimensional stone before actual extraction, J. Min. Sci. 43 (2007) 75–80. doi:10.1007/s10913-007-0008-4.

[39] R. Yarahmadi, R. Bagherpour, S.G. Taherian, L.M.O. Sousa, Discontinuity modelling and rock block geometry identification to optimize production in dimension stone quarries, Eng. Geol. 232 (2018) 22–33. doi:10.1016/j.enggeo.2017.11.006.

[40] M. Fernández-de Arriba, M.E. Díaz-Fernández, C. González-Nicieza, M.I. Álvarez-Fernández, A.E. Álvarez-Vigil, A computational algorithm for rock cutting optimisation from primary blocks, Comput. Geotech. 50 (2013) 29–40. doi:10.1016/j.compgeo.2012.11.010.

[41] S. Mosch, D. Nikolayew, O. Ewiak, S. Siegesmund, Optimized extraction of dimension stone

blocks, Environ. Earth Sci. 63 (2011) 1911–1924. doi:10.1007/s12665-010-0825-7.

[42] M.M. Demarco, P. Oyhantcabal, K.-J. Stein, S. Siegesmund, Granitic dimensional stones in Uruguay: evaluation and assessment of potential resources, Env. Earth Sci. 69 (2013) 1397–1438. doi:10.1007/s12665-012-2027-y.

[43] M.I. Álvarez-Fernández, C. González-Nicieza, A.E. Álvarez-Vigil, L.R. Alejano, Geometrical design of ornamental stone slabs cutting using the neutral region concept, Int. J. Rock Mech. Min. Sci. 52 (2012) 31–39. doi:10.1016/j.ijrmms.2012.01.012.

[44] P. Guigue, O. Devillers, Fast and robust triangle-triangle overlap test using orientation predicates, J. Graph. Tools. 8 (2003) 25–32. doi:10.1080/10867651.2003.10487580.

[45] D. Vidić, I. Galić, B. Farkaš, The profitability of dimension stone deposit exploitation in relation to the coefficient of utilization, Mining-Geology-Petroleum Eng. Bull. 25 (2012) 123–130.

[46] N. Careddu, G. Siotto, Promoting ecological sustainable planning for natural stone quarrying. The case of the Orosei marble producing area in Eastern Sardinia, Resour. Policy. 36 (2011) 304–314. doi:10.1016/j.resourpol.2011.07.002.

[47] G. Marras, G. Siotto, J.L. Parra, N. Careddu, Potential applications of waste material deriving from marble processing plants, in: 7th Int. Marble Nat. Stones Congr. Turkey (Mersem VII), 14–15 October 2010, Afyonkarahisar, Turkey, 2010: pp. 55–61.

[48] M. Lokeshwari, K.S. Jagadish, Eco-friendly use of granite fines waste in building blocks, Procedia Environ. Sci. 35 (2016) 618–623. doi:10.1016/j.proenv.2016.07.049.

[49] M.E. Allam, E.S. Bakhoum, G.L. Garas, Re-use of granite sludge in producing green concrete, ARPN J. Eng. Appl. Sci. 9 (2014) 2731–2737.

[50] Bourke P., PLY - Polygon File Format, (2011). http://paulbourke.net/dataformats/ply/ (accessed March 19, 2018).

[51] ParaView website, (n.d.). http://www.paraview.org/ (accessed May 1, 2018).

[52] OpenMP website, (n.d.). http://www.openmp.org/ (accessed May 1, 2018).

Appendix A

The directives of the working mode, the bounding domain, output options of SlabCutOpt are included in the SlabCutOpt.par file. Keywords are briefly resumed in the given example file below.

```
#SlabCutOpt parameters file
# Block domain definition
x_max=+0.9 #
x_min=+0.0 #
y_max=+2.0 #
y_min=+0.0 #
z_max=+1.1 #
z_min=+0.0 #
#Cutting slab dimensions
dim_x=0.41 # Distance between cutting planes in x direction
dim_y=0.21 # Distance between cutting planes in y direction
dim_z=0.04 # Distance between cutting planes in z direction
cut_saw_thickness=0.01 # Saw thickness (meter)
#Space of solutions
#angles (radiant)
theta_step=1.570796327 #
theta_max=1.570796328 #
phi_step=1.570796327 #
phi_max=1.570796328 #
psi_step=1.570796327 #
psi_max=1.570796328 #
#displacement (meters)
dx_step=0.05 #
dy_step=0.05 #
dz_step=0.05 #
#Options
read_slab_dimensions=1 #0: read only the dimensions of the single slab indicated here;
1: consider also a list of different dimensions of slabs
read_bound=0 #0: the ply file describing the faces of the block in a form of triangles
rotation_method=1 #0: Euler rotation; 1: Cartesian axis rotation
BiDimensional=0 # #0: 3D operation; 1: 2D operation
write_vtu=1 #0: no vtu file in output; #1: for each slab size within all the tested
displacements, a slab.vtu file is generated; #2: only the solution of the maximum
number of non-intersected slabs for each slab size
read_PLY_FileList=1 #0: Read the fracture set from "test_fractures.ply"; 1 read the
PLY_FileList.dat for using several PLY files of discontinuities
end=end
```

Appendix B

The PLY file format readable by SlabCutOpt is a simplified version of the more general PLY file format, such as the example below. Each element must have 3 vertices (a triangle in the 3D space). The fixed characters are presented in italic, while the geometrical parameters for a discontinuity description are presented in bold. After the header, a number specified in [*element vertex*] indicates the coordinates of the vertices, then the following [*element face*] lines define the number of vertices (*3*) and the vertices index of each triangle. It is worth mentioning that, in the more general PLY file format, the number of vertices can be higher for polygonal elements.

ply
format ascii 1.0
comment example of a fracture represented by 2 triangles
element vertex **4**
property float x
property float y
property float z
element face **2**
property list uchar int vertex_index
end_header
0.000 2.000 0.553
0.450 2.000 0.553
0.000 0.000 0.583
0.450 0.000 0.599
3 0 1 2
3 1 2 3

Appendix C

The PLY_FileList.dat input file must contain the list of the ply files of the modelled discontinuities. No header is allowed. Below is an example of PLY_FileList.dat.

block_fracturepink_g.ply
block_fracturepink_h.ply
block_fracturepink_k.ply
brown_frac.ply
extended_void_blue.ply
purple_frac.ply
red_frac.ply
single_void.ply
turquoise_frac.ply
yellow_frac.ply

Appendix D

The slab_dimensions.dat input file must contain the list of the different sizes of slabs that the algorithm must test. Below is an example of slab_dimensions.dat. The order of the columns, from left to right, is dim_x, dim_y, dim_z. The dimensions of the slabs must be increased by the cut_saw_thickness for geometrical considerations in the algorithm.

```
0.41    0.21    0.025
0.51    0.26    0.025
0.41    0.21    0.03
0.51    0.26    0.03
0.61    0.31    0.025
0.31    0.31    0.025
0.41    0.41    0.025
0.61    0.46    0.025
0.46    0.46    0.025
0.49    0.49    0.025
0.61    0.31    0.03
0.31    0.31    0.03
0.41    0.41    0.03
0.61    0.46    0.03
0.46    0.46    0.03
0.49    0.49    0.03
```

Appendix E

The results file is an ASCII file containing the optimization results. The first part lists the dimension of the slabs tested, as shown in the example below. Following, a list of solutions is provided for each size. The list consists of 12 columns, from left to right there are: the order number of iteration, dim_x, dim_y, dim_z, theta, phi, psi, the total number of slabs inside the block, and the number of intersected slabs.

Optimization results:

```
Number of tested dimensions of slabs: 37

[0] dim_x= 0.410000 dim_y= 0.210000 dim_z= 0.025000
[1] dim_x= 0.510000 dim_y= 0.260000 dim_z= 0.025000
.. .. .. .. .. .. .. .. .. .. .. ..
[n] dim_x= 0.260000 dim_y= 1.260000 dim_z= 0.040000

Results_for_slab_[0]
..   ...   ...   ...   ...   ...   ...   ...   ...   ...   ...  ...
..   ...   ...   ...   ...   ...   ...   ...   ...   ...   ...  ...
..   ...   ...   ...   ...   ...   ...   ...   ...   ...   ...  ...
Results_for_slab_[1]
..   ...   ...   ...   ...   ...   ...   ...   ...   ...   ...  ...
..   ...   ...   ...   ...   ...   ...   ...   ...   ...   ...  ...
..   ...   ...   ...   ...   ...   ...   ...   ...   ...   ...  ...

764 0.510000 0.260000 0.025000 1.570796 1.570796 0.000000 -0.205000 -0.030000 -0.012500 426 121
765 0.510000 0.260000 0.025000 1.570796 1.570796 0.000000 -0.205000 0.020000 -0.012500 422 70
766 0.510000 0.260000 0.025000 1.570796 1.570796 0.000000 -0.205000 0.070000 -0.012500 422 75
767 0.510000 0.260000 0.025000 1.570796 1.570796 0.000000 -0.205000 0.120000 -0.012500 422 88
768 0.510000 0.260000 0.025000 1.570796 1.570796 0.000000 -0.155000 -0.130000 -0.012500 425 106
769 0.510000 0.260000 0.025000 1.570796 1.570796 0.000000 -0.155000 -0.080000 -0.012500 425 113

..   ...   ...   ...   ...   ...   ...   ...   ...   ...   ...  ...
..   ...   ...   ...   ...   ...   ...   ...   ...   ...   ...  ...
..   ...   ...   ...   ...   ...   ...   ...   ...   ...   ...  ...
 Results_for_slab_[n]
..   ...   ...   ...   ...   ...   ...   ...   ...   ...   ...  ...
```